First Principle Fluid Modelling of Neoclassical Tearing Modes and of their Control

P. Maget[1], O. Février[1], X. Garbet[1], G. Giruzzi[1], H. Lütjens[2], J-F Luciani[2], P. Beyer[3], J. Decker[4], O. Sauter[4], E. Lazzaro[5], S. Nowak[5], M. Reich[6], the Asdex-Upgrade Team and the MST1 Eurofusion team[1]

[1] CEA, IRFM, F-13108 Saint Paul-lez-Durance, France.
[2] Centre de Physique Théorique, Ecole Polytechnique, CNRS, France.
[3] Aix-Marseille Université, CNRS, PIIM UMR 7345, 13397 Marseille Cedex 20, France.
[4] École Polytechnique Fédérale de Lausanne, SPC, CH-1015 Lausanne, Switzerland.
[5] Istituto di Fisica del Plasma P.Caldirola, CNR, Milano, Italy.
[6] Max-Planck-Institut für Plasmaphysik, D-85748 Garching, Germany.

e-mail contact of main author: patrick.maget@cea.fr

Abstract The confinement degradation of Tokamak plasma by magnetic islands motivates numerous approaches in order to better understand their dynamics and possible suppression. We report here on the characterization of island dynamics using a consistent two-fluid implementation of neoclassical friction forces in the framework of the toroidal Magneto-Hydro-Dynamic model of the XTOR code [1, 2, 3], as well as on first principles modelling of island stabilization by Electron Cyclotron Current Drive (ECCD) [4, 5].

1 Drift-neoclassical model and insights on NTM drive

The importance of drift physics in the dynamics of tearing modes [6, 7, 8] claims for a consistent implementation of neoclassical forces in global fluid modelling of Neoclassical Tearing Modes (NTM), instead of using an ad-hoc bootstrap current proportional to the pressure gradient. Following earlier works [9], this implementation has been achieved in the toroidal nonlinear MHD code XTOR-2F [2, 3]. The bootstrap current now emerges from the neoclassical drive exerted on ion and electron poloidal flows through a friction force. In the absence of magnetic perturbations, the equilibrium bootstrap is formally consistent with the standard flux averaged neoclassical theory [10], and agrees well with formulaes derived from the Fokker-Planck equation [11]. The (2,1) island that is studied rotates in the electron direction, as predicted by theory [12]. However, several important aspects change our view on NTM generation when compared to the formalism of the extended Rutherford equation, as shown in the following for a test case with circular cross section, $q = 2$ at $\sqrt{\psi} = 0.5$, and a reference normalized beta of 0.84.

First, the island dynamics can be perturbed by bursts of small scale reconnections (similar to plasmoids) when neoclassical friction is introduced, if dissipation mechanisms (diffusivity or viscosity) are low. This is shown in figure 1, where $M^{1/4}$ (with M the magnetic

[1]See appendix of H. Meyer et.al. (OV/P-12) Proc. 26th IAEA Fusion Energy Conf. 2016, Kyoto, Japan

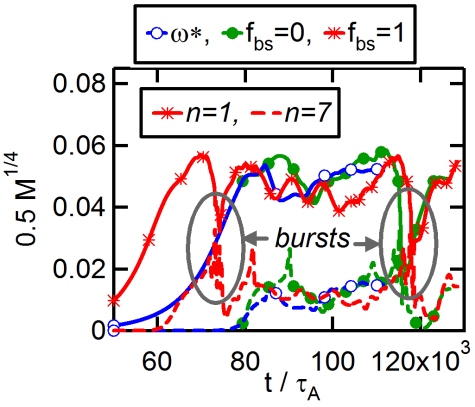

Figure 1: *Dynamics of $M^{1/4}$ with M the magnetic energy of the (2,1) mode, for the drift and the full model with and without bootstrap current ($f_{bs} = 1$ / 0).*

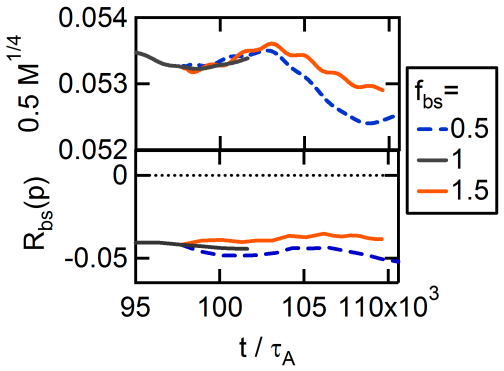

Figure 2: *Dynamics of $M^{1/4}$ with M the magnetic energy of the (2,1) mode, for different amplifications (f_{bs}) of the bootstrap current.*

energy, this quantity represents the island width) is plotted as a function of time for the $n = 1$ and $n = 7$ modes for the drift (ω^*) and the neoclassical models.

Second, the increase of the island size when increasing independently the local bootstrap current density is extremely weak (few % of the Rutherford prediction), for the test equilibrium that is used. This appears to be related with the fact that the connection between diamagnetic flows and the bootstrap current is now mediated by the $\mathbf{E} \times \mathbf{B}$ flow. This connection can be evaluated by computing the correlation between the perturbed bootstrap current density and the perturbed pressure gradient, using the measure:

$$R(f,g) = \left(\int dV\, fg\right) / \left[\left(\int dV\, f^2\right)^{1/2} \left(\int dV\, g^2\right)^{1/2}\right] \tag{1}$$

with $f \equiv [J_{bs,\varphi}]_{n\neq 0}$ and $g \equiv [-\partial_y p]_{n\neq 0}$ with p the pressure and $y \equiv \sqrt{\psi}$ the radial coordinate. We note $R_{bs}(p) = R(f,g)$. With the ad-hoc bootstrap model ($J_{bs} \propto \nabla p$), we have naturally $R_{bs}(p) = 1$. In the following, we have damped the bursts by using a higher perpendicular transport coefficient ($\times 2$) compared to figure 1. The correlation $R_{bs}(p)$ is found to be close to zero, and even slightly negative for the reference equilibrium: the bootstrap is uncorrelated with the pressure perturbation and does not participate in the island current (figure 2). When varying the bootstrap current by an ad-hoc factor f_{bs} in Ohm's law, this correlation is marginally increased : this explains the reduced impact that is observed on the saturation.

In order to further investigate the transition between this regime where neoclassical effects weakly contributes to the saturation, and the NTM branch, we have performed scans on plasma density, and on plasma beta, acting simultaneously on drift and neoclassical physics in different ways. Increasing the density N (at constant pressure) reduces drift

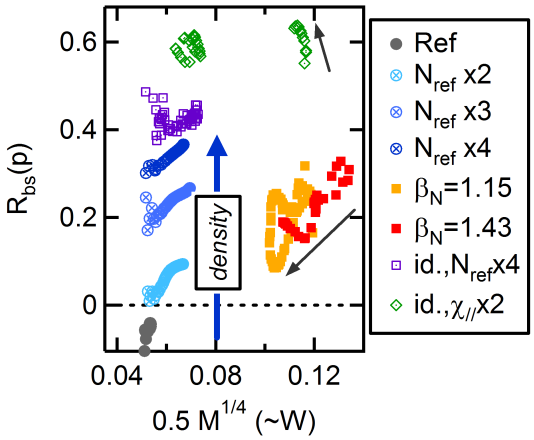

Figure 3: *Coupling $R_{bs}(p)$ between bootstrap current and pressure, as a function of $M^{1/4}$ ($\sim$ island width).*

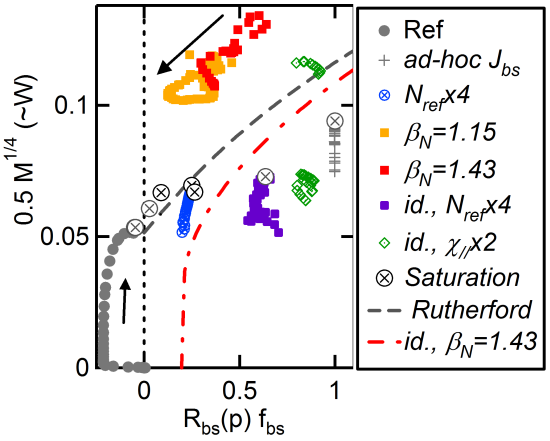

Figure 4: *Island width (represented by $M^{1/4}$) as a function of the effective bootstrap contribution $R_{bs}(p) \times f_{bs}$.*

effects ($\omega^* \propto 1/N$) and the equilibrium bootstrap current (because of collisionality). Since the latter does not contribute a lot to the island saturation at the reference β, we essentially see the consequence of reducing drift effects, which results in a larger saturation [6, 8]. Although the bootstrap doesn't participate significantly in the saturation size, the relation $R_{bs}(p)$ between the bootstrap and pressure perturbations becomes stronger. This can be explained by the drmatic change of the ion neoclassical friction μ_i (normalized to the Alfvén time), that is increased by an order of magnitude when the density is increased by a factor of 4. This forces the electrostatic potential towards its neoclassical value that is a combination of drift velocities (figure 3). In the β-scan, drift effects, bootstrap current, as well as toroidal stabilization are increased at the same time (the mode is linearly stable above $\beta_N = 1.29$). We start most simulations by inserting a seed (this is mandatory for stable cases), and these seeded cases evidence the fact that $R_{bs}(p)$ increases also with the island size (figure 3). When the parallel diffusivity $\chi_\parallel$ is increased, the characteristic transport width decays [13], helps flattening the bootstrap current inside the island, and increases the connection between the bootstrap and pressure perturbations. The results are summarized in figure 4, where the quantity $M^{1/4}$, representing the island size, is plotted against the effective bootstrap contribution $R_{bs}(p) \times f_{bs}$, with $f_{bs} = J_{bs}/J_{bs}^{ref}$, J_{bs} being the equilibrium bootstrap current on $q = 2$ for a given case and J_{bs}^{ref} for the reference case. Taking this correction into account, a stability diagram can be derived and compared with the Rutherford equation prediction (including curvature stabilization), adjusted at $R_{bs}(p) \times f_{bs} = 0$. Although the range covered by our study is so far reduced, we still find that the saturation size depends weakly on the bootstrap current, at least up to $R_{bs}(p) \times f_{bs} = 0.8$. With the ad-hoc bootstrap model, the island saturates at a larger size, but still below the analytical prediction.

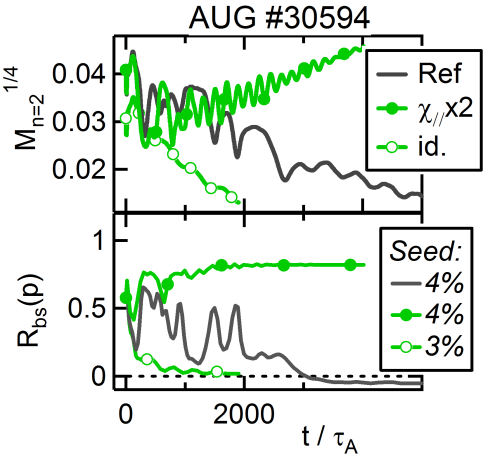

Figure 5: *(3,2) NTM seeding. Top: Island width for different seed sizes; bottom: coupling between bootstrap and pressure.*

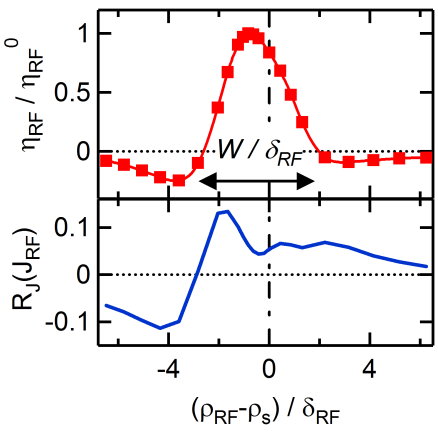

Figure 6: *η_{RF} (top) and $R_J(J_{RF})$ (bottom) as a function of misalignement, from XTOR simulations.*

A first application of the neoclassical model to a (3,2) NTM is shown in figure 5. Here, a seed is introduced on an experimental equilibrium from Asdex-Upgrade (#30594). The coupling of the bootstrap current with pressure is varied by changing the characteristic transport width through the parallel diffusivity $\chi_\parallel$. The NTM is not triggered for a seed of 4% of the minor radius and $\chi_\parallel/\chi_\perp = 10^7$, while it grows when $\chi_\parallel$ is amplified by a factor 2. This corresponds indeed to larger coupling $R_{bs}(p)$, an interpretation that is in line with the results shown in figure 3.

2 Island control by ECCD

The control of a magnetic island by a localized current drive is investigated by adding a source term in the Ohm's law and a propagation equation for the parallel current [4]. We assume a parallel diffusion of the RF current along field lines that ensures an almost constant value on flux surfaces for arbitrary magnetic configuration, a distribution that is consistent with the result of a more adequate convective propagation process when the island rotation is not too fast [14]. The measure of the RF impact on the island can be computed using $R(f,g)$, with $f \equiv -J_{\varphi,n\neq 0}$ and $g \equiv J_{RF,\varphi}$, that we will note as $R_J(J_{RF})$. When the RF current compensates for the island current, this measure is positive, and it is negative in the opposite case. The importance of the 3D localization of the source term is illustrated by two phenomena where the ability of the island to adjust its phase is evidenced. The first one is the flip instability [15]: a static island will adjust its phase so as to grow when the RF source is initially focussed on its O-point. The second is the growth of a RF-driven island when the source is localized at a resonant surface in a stable plasma.

Both phenomena are mitigated by the rotation of the island. The efficiency η_{RF} of the RF control, as defined in [16], is computed from resistive MHD simulations by considering the initial jump of the island width (before any flip) and compared with analytical predictions. We recover the decreased stabilization efficiency as the source width δ_{RF} becomes large compared with the island width, as well as the detrimental effect of radial misalignment, including the asymmetry associated with that of the island [17] (figure 6).

In addition to the implementation of the RF source term, a basic controller has been added in order to investigate various control strategies:

- the preemption aimed at avoiding the birth of an island;
- the radial sweeping aimed at mitigating the misalignment risk [18], that has been successfully tested on TCV and Asdex-Upgrade [2];
- the modulation aimed at mitigating situations with a too broad current deposition profile [19].

as well as combinations of these techniques in order to obtain a robust control method. We perform this study on the basis of a classically unstable (2,1) tearing mode, and with the resistive MHD model [5], for a source width δ_{RF} of about 13% of the minor radius.

Regarding preemption, we verify that RF current and its action on equilibrium are able to stabilize linearly a tearing mode, but the misalignment of a narrow source can have deleterious consequences [20]. When combined with radial sweeping, we find that preemption can prevent the growth of the island over a wide region, at the cost of a larger RF current (figure 7).

The radial sweeping applied to a saturated island mitigates as expected the risk of misalignement, but the minimum island width that is obtained is larger than with a perfectly aligned source (note that in the case of a metastable mode, it would be sufficient to go below the critical width). The dynamics of the island for a RF current representing 1% of the plasma current is shown in figure 8 for a well aligned fixed source, for a sweep covering $\pm 5\%$ of the minor radius, and for a sweep combined with modulation or FADIS (see later). Looking at the radial shape of the RF stabilization efficiency, it is clear that an efficient sweep should not spend too much time in the two destabilizing wells located outside $W/(2\delta_{RF})$. Also, due to the asymmetry of $\eta_{RF}(\rho_{RF})$ (this asymmetry is even more pronounced when considering $R_J(J_{RF})$), it is better to spend time on the outer side of the island than on the inside. Since we do not know presicely the position of the resonance, we envisage the case where the sweep is not well centered, but outside the resonance. The minimum island size is plotted in figure 9 as a function of the sweep amplitude for a well centered and a misaligned sweep. Due to the asymmetry, a sweep that is misaligned by $+5\%$ can be more efficient than a well centered one, because it will explore less the destabilizing region that is on the inner part.

[2] see summary contributions at this conference

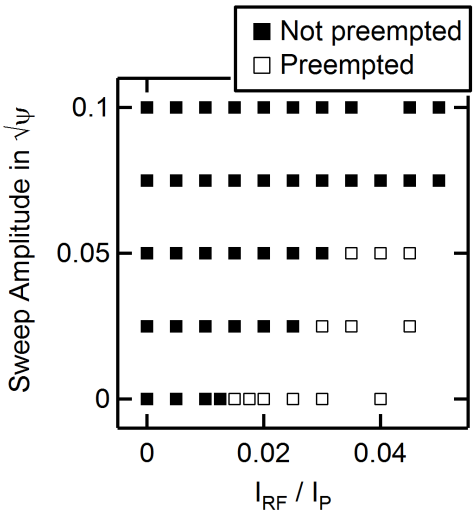

Figure 7: *Amplitude of the sweep as a function of the RF current for getting pre-emption.*

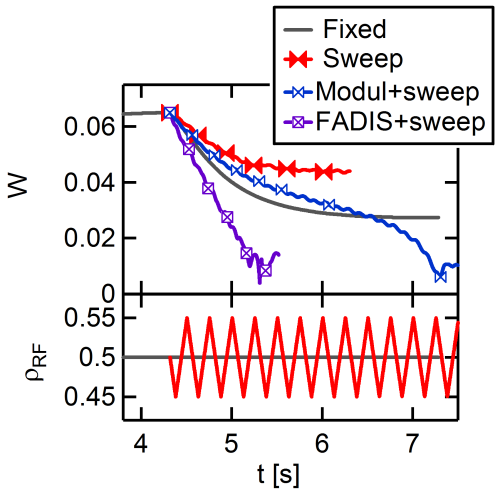

Figure 8: *Island dynamics for a fixed and a sweeping RF source, including modulation techniques ($\delta_{RF}/W_{sat} = 1.4$).*

In order to evaluate a given control strategy, we define a gain relative to a fixed, continuous and well aligned source:

$$G = (W_{sat} - W_{min}) \,/\, (W_{sat} - W_0) \tag{2}$$

where W_{sat} is the saturation width of the island, W_{min} the minimum width reached during the island control after $\Delta t = T_{min}$ and W_0 the island width obtained with the fixed, continuous and well aligned source that is used as a reference. This gain is unity for this reference case, goes to zero if the control method does not change the island width, and is above unity when the method is more efficient than the reference. The results of simulations is summarized in figure 10 for a source that is larger than the saturated island width ($\delta_{RF}/W_{sat} = 1.4$). The gain obtained with the simple sweep is moderate (≈ 0.5), but it allows avoiding the negative gain of the misaligned fixed source. A well-positioned modulation (50% duty cycle) increases the gain to $G \approx 1.7$ (the island is almost completely suppressed) and reduces the time delay by about 60%. When combined with a centered sweep, the gain remains high at the cost of a time delay that is not reduced. We finally investigate the FADIS [3] method [21], that allows hitting continuously the island O-point by modulating alternatively on two launchers focussed on opposite island phases (one is directed towards the O-point when the other sees the X-point). With this method, the island is also completely suppressed, with a time delay that is half that of the centered modulation technique. Moreover, the time delay remains low even when using the sweep, because the island is rapidely suppressed at the first crossings of the island position.

[3] FAst DIrectional Switch

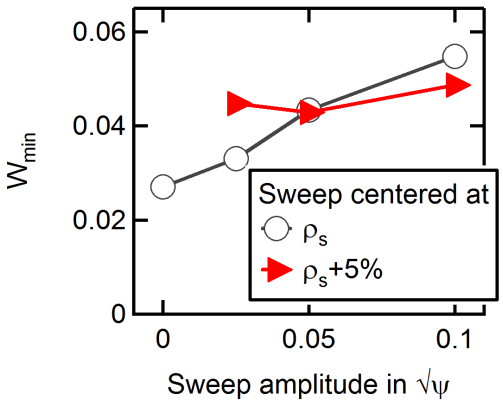

Figure 9: *Minimum island width as a function of the sweep amplitude for a well centered and a sweep misaligned by* $+5\%$ *(*$\delta_{RF}/W_{sat} = 1.4$*).*

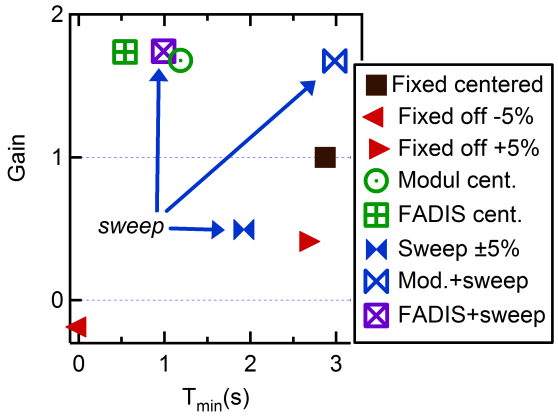

Figure 10: *Gain as a function of the time needed for reaching* W_{min}*, for various control strategies (*$\delta_{RF}/W_{sat} = 1.4$*).*

3 Summary

We have presented results on the dynamics of neoclassical tearing modes, investigated using a drift-neoclassical MHD model implemented in the full MHD toroidal code XTOR-2F, and results on island stabilization strategies using the resistive MHD model. We showed that drift physics gives a droplet shape to magnetic islands, and that neoclassical forces can drive island filamentation if dissipation is low enough. We find that the bootstrap current perturbation is not correlated with the pressure perturbation when the island size is small while it is fully correlated when using an ad-hoc bootstrap current proportional to the pressure gradient. The contribution of the bootstrap current to saturation has been shown to be mitigated by its electrostatic contribution, that does not necessarily follow the neoclassical drive, and does not reinforce the island current when neoclassical friction or island size are small.

Regarding island control by a current source, we validated the code against analytical results and investigated control strategies using a simple controller. We find that radial sweeping can efficiently mitigate the risk of misalignment. This technique can be significantly improved by combining it with a simple modulation, but the best results are obtained using an alternate modulation allowing a nearly continuous O-point hitting (known as the FADIS technique).

Acknowledgments

This work has been carried out within the framework of the EUROfusion Consortium and the French Research Federation for Fusion Studies and has received funding from the Euratom research and

training programme 2014-2018 under grant agreement No 633053. We benefited from HPC resources from GENCI (project 056348), IFERC (project MaCoToP) and from Aix-Marseille Université project Equip@Meso (ANR-10-EQPX-29-01) of the program "Investissements dAvenir" supervised by the Agence Nationale pour la Recherche. This work is part of the project AMICI funded by the Agence Nationale pour la Recherche (ANR-14-CE32-0004-01). The views and opinions expressed herein do not necessarily reflect those of the European Commission.

References

[1] LÜTJENS H. ET AL. *Journal of Computational Physics* **229** (2010) 8130 .

[2] MELLET N. ET AL. *Nuclear Fusion* **53** (2013) 043022.

[3] MAGET P. ET AL. *Nuclear Fusion* **56** (2016) 086004.

[4] FÉVRIER O. ET AL. *Plasma Physics and Controlled Fusion* **58** (2016) 045015.

[5] FÉVRIER O. ET AL. Theory of Fusion Plasmas, Joint Varenna-Lausanne International Workshop, Varenna (Italy) (2016). *Submitted to Plasma Phys. and Cont. Fusion*

[6] YU Q. *Nuclear Fusion* **50** (2010) 025014.

[7] MESHCHERIAKOV D. ET AL. *Physics of Plasmas* **19** (2012) 092509.

[8] MESHCHERIAKOV D. ET AL. *Physics of Plasmas* **21** (2014) 012516.

[9] CALLEN J.D. *Physics of Plasmas* **17** (2010) 056113.

[10] HIRSHMAN S.P. ET AL. *Nucl. Fusion* **21** (1981) 1079.

[11] SAUTER O. ET AL. *Physics of Plasmas* **6** (1999) 2834. SAUTER O. ET AL. *Physics of Plasmas* **9** (2002) 5140.

[12] WAELBROECK F.L. *Plasma Physics and Controlled Fusion* **49** (2007) 905.

[13] FITZPATRICK R. *Physics of Plasmas* **2** (1995) 825.

[14] WESTERHOF E. ET AL. *Physics of Plasmas (1994-present)* **21** (2014) 102516.

[15] BORGOGNO D. ET AL. *Physics of Plasmas (1994-present)* **21** (2014) 060704.

[16] HEGNA C.C. ET AL. *Physics of Plasmas* **4** (1997) 2940.

[17] LAZZARI D.D. ET AL. *Plasma Physics and Controlled Fusion* **53** (2011) 035020.

[18] KIM D. *Real-Time Control of Sawteeth and NTMs in TCV and ITER*. Theses, Ecole polytechnique fédérale de Lausanne EPFL (2015).

[19] MARASCHEK M. ET AL. *Phys. Rev. Lett.* **98** (2007) 025005.

[20] PLETZER A. ET AL. *Physics of Plasmas* **6** (1999) 1589.

[21] KASPAREK W. ET AL. *Nuclear Fusion* **56** (2016) 126001.